REPORT DOCUMENTATION PAGE

Form Approved OMB NO. 0704-0188

1. AGENCY USE ONLY (Leave Blank)	2. REPORT DATE:	3. REPORT TYPE AND DATES COVERED Final Report 1-Jul-2004 - 18-Nov-2005

4. TITLE AND SUBTITLE
Mid-infrared Quantum Dot Cascade Lasers

5. FUNDING NUMBERS
W911NF0410313

6. AUTHORS
Dennis G. Deppe

8. PERFORMING ORGANIZATION REPORT NUMBER

7. PERFORMING ORGANIZATION NAMES AND ADDRESSES
University of Texas - Austin
Office of Sponsored Projects
101 E. 27th Street
Austin, TX 78712 -

9. SPONSORING/MONITORING AGENCY NAME(S) AND ADDRESS(ES)
U.S. Army Research Office
P.O. Box 12211
Research Triangle Park, NC 27709-2211

10. SPONSORING / MONITORING AGENCY REPORT NUMBER
46663-PH.1

11. SUPPLEMENTARY NOTES
The views, opinions and/or findings contained in this report are those of the author(s) and should not contrued as an official Department of the Army position, policy or decision, unless so designated by other documentation.

12. DISTRIBUTION AVAILIBILITY STATEMENT
Approved for Public Release; Distribution Unlimited

12b. DISTRIBUTION CODE

13. ABSTRACT (Maximum 200 words)
The abstract is below since many authors do not follow the 200 word limit

14. SUBJECT TERMS
semiconductor lasers, mid infrared, quantum dots, unipolar injection

15. NUMBER OF PAGES
Unknown due to possible attachments

16. PRICE CODE

17. SECURITY CLASSIFICATION OF REPORT	18. SECURITY CLASSIFICATION ON THIS PAGE	19. SECURITY CLASSIFICATION OF ABSTRACT	20. LIMITATION OF ABSTRACT
UNCLASSIFIED	UNCLASSIFIED	UNCLASSIFIED	UL

NSN 7540-01-280-5500

Standard Form 298 (Rev .2-89)
Prescribed by ANSI Std.
239-18 298-102

Report Title

InP-Based Quantum Dot Cascade Lasers

ABSTRACT

This project conducts research necessary to design, growth, and demonstrate laser action in semiconductor quantum dots based on unipolar injection. The designs use new injection techniques that account for the electron wavefunction symmetries based on the height-to-base aspect ratios of self-organized quantum dots. The material systems being explored are InAs quantum dots grown within either GaAs-based or InP-based heterostructures. While GaAs-based quantum dots are better developed, InP-based quantum dots benefit from better conduction band alignment in the InAlAs/InGaAs heterostructures needed for mid-infrared sources.

List of papers submitted or published that acknowledge ARO support during this reporting period. List the papers, including journal references, in the following categories:

(a) Papers published in peer-reviewed journals (N/A for none)

Number of Papers published in peer-reviewed journals: 0.00

(b) Papers published in non-peer-reviewed journals or in conference proceedings (N/A for none)

D.G. Deppe and M. Gobert, "Quantum Dot Heterostructure Based on Electron Tunneling for Infrared Cascade Lasers," SPIE Conference Proceedings on Laser Source and System Technology for Defense and Security, March 28 - April 1, 2005, Orlando, FL.

Number of Papers published in non peer-reviewed journals: 1.00

(c) Papers presented at meetings, but not published in conference proceedings (N/A for none)

(Invited) D.G. Deppe, "Quantum Dot Quantum Cascade Lasers," International Workshop on Quantum Cascade Lasers 2004, January 5-8, 2004, Seville, Spain.

Number of Papers not Published: 0.00

(d) Manuscripts

Number of Manuscripts: 0.00

Number of Inventions:

Graduate Students

NAME	PERCENT_SUPPORTED	
Mathilde Gobet	0.50	No
FTE Equivalent:	**0.50**	
Total Number:	**1**	

Names of Post Doctorates

NAME	PERCENT_SUPPORTED	
Sabine Freisem	0.10	No
FTE Equivalent:	**0.10**	
Total Number:	**1**	

Names of Faculty Supported

NAME	PERCENT_SUPPORTED	National Academy Member
Dennis Deppe	0.10	No
FTE Equivalent:	**0.10**	
Total Number:	**1**	

Names of Under Graduate students supported

NAME	PERCENT_SUPPORTED
FTE Equivalent:	
Total Number:	

Names of Personnel receiving masters degrees

NAME
Total Number:

Names of personnel receiving PHDs

NAME
Total Number:

Names of other research staff

NAME	PERCENT_SUPPORTED	
Terry Mattord	0.05	No
FTE Equivalent:	**0.05**	
Total Number:	**1**	

Sub Contractors (DD882)

Inventions (DD882)

Quantum Dot Cascade Heterostructure Based on In-Plane Dipole Moments for Unipolar Infrared Cascade Lasers

Mathilde Gobet and Dennis G. Deppe

Microelectronics Research Center
Department of Electrical and Computer Engineering
The University of Texas at Austin, Austin, Texas 78712-1084

1. Introduction

Room temperature, high efficiency infared laser sources can open up new applications such as medical imaging, sensing, inspection, and security surveillance. However, obtaining room temperature operation sources that are compact, robust, and operate with high efficiency has been difficult. The semiconductor is one of the most attractive materials for such sources, since it can provide direct electrical-to-optical (infrared) power conversion.

Unipolar quantum cascade semiconductor lasers based on the intersubband electron transitions of planar quantum wells can operate in the mid and far-infrared spectrum [1]-[2]. Especially at the shorter wavelengths of 4 to 10 μm, room temperature operation has been demonstrated suggesting these semiconductor devices could be useful for new surgery and medical spectroscopy techniques, as well as monitoring of chemical species and free space communication due to the low absorption atmospheric window. The advantages of unipolar quantum cascade lasers over traditional interband electron-hole lasers are their reliance on well developed GaAs- and InP-based heterostructure materials that can provide high reliability, compact, and low cost devices.

However, planar quantum well unipolar lasers are intrinsically limited by the electronic density of states set by the quantum dimensionality of the active material. This density of states is a continuum in energy, allowing phonon transitions to dominate the radiative recombination between intersubband quantum states of different energy. The result of the dominant phonon emission in the intersubband transitions is a very short nonradiative relaxation time that is not linked to material quality, but due to the electron-longitudinal phonon scattering. The phonon emission times of ~1 ps as compared to photon emission times of >10 ns results in very poor radiative efficiency below threshold, even at low temperature, and gives rise to threshold current densities that are increased by several orders of magnitude over that which would be set by radiative recombination. Furthermore, the radiative selection rules in planar quantum wells prevent direct surface emission, since the dipole moment is polarized normal to the well plane, i.e. along the confinement direction of the well. This eliminates the prospect of a vertical-cavity surface-emitting laser in a unipolar planar quantum well device.

Quantum dots (QDs) that provide three-dimensional quantum confinement and lead to fully discrete quantum states have the intrinsic physics to overcome the limitations of planar quantum well unipolar lasers. Due to their discrete atom-like quantum states, QDs suppress nonradiative relaxation via longitudinal phonons because this transition no longer conserves energy. This is the same behaviour exhibited by electron-hole lasers, in which radiative recombination dominates transitions and provides low threshold current density. Therefore when fully developed, a QD unipolar cascade laser (QDCL) is expected to reduce threshold

current densities as compared to planar quantum well lasers by potentially orders of magnitude, and exhibit much less temperature sensitivity. Another important feature of a QDCL is the ability to produce an in-plane dipole moment due to lateral confinement, leading to opportunity for surface emission and a vertical cavity surface emitting laser that may exhibit low power consumption and scaling to two-dimensional arrays. Here it is the potential for resonant periodic gain that makes the unipolar cascade approach of a QDCL so attractive.

There have been different proposals and attempts to achieve mid-infrared intraband electroluminescence from QDs [3]-[5], but these have not to date produced convincing evidence of radiative transitions that arise from the QDs. These attempts have generally followed the general planar quantum well cascade approach and proven ineffective at producing efficient light emission, and especially surface emission. Although the operation of the QD heterostructures attempted so far is not too clear, we propose that this failure in efficient light emission has resulted from the lack of appreciation of how the intrinsic physics differ for electron confinement and transitions in QDs as opposed to planar quantum wells. Electron injection and tunnelling phenomenon change dramatically when a quasi-zero-dimensional system such as the self-organized QD is coupled to a planar heterostructure superlattice that exhibits two degrees of freedom in the electron motion. As we discuss below, in some cases, the electrons confined in QD quantum states cannot be blocked at all by planar superlattices, while in other cases the blocking is less effective than in fully planar heterostructures due to electron diffraction.

In this paper we describe the physics of the QD energy levels that we propose can be used for a new approach in unipolar lasers. This new approach is based on electron capture due to energy relaxation into discrete QD quantum states, and that can exhibit high efficiency luminescence due to the elimination or reduction of phonon emission. We describe engineering the confinement mechanism in the QD quantum states to obtain three-dimensional confinement, and how to couple these states to planar superlattices to allow rapid electron escape from lower energy levels. We then describe our initial experiments aimed at realizing these new types of QD heterostructures that could lead to QD cascade lasers.

2. Basic Principles of a QD Gain Stage for Transverse Electric Field Emission

The main problem in the realization of a QD QCL is the fact that, opposed to the QW where a superlattice permits electron confinement, electrons in QD quantum states are not necessarily confined by a planar superlattice. The explanation for the lack of confinement is given using the schematic illustrated in Fig. 1. For a typical self-organized QD the height-to-base aspect ratio establishes the two lowest energy quantum states with their energy separation set by the base dimension. For the aspect ratio shown, and assuming the Hamiltonian describing the quantum confinement leads to approximately spatially separable solutions, the two lowest quantum states are due to the spatial eigensolutions that differ in the x-y plane, while they exhibit the same spatial dependence in the z-direction normal to the superlattice. Because the spatial dependence in the z-direction for E_0 and E_1 are identical, an electron that occupies the higher energy level of E_1 cannot be blocked by the superlattice in the z-direction that would pass the electron from E_0 into the superlattice miniband. In this case, superlattices are ineffective in producing electronic confinement in QDs.

Although higher energy states may exist in the QD heterostructure illustrated in Fig. 1 with orthogonal z-dependence to E_0 in which their electron transport would be blocked, these states

are less desirable for operation of a QD cascade laser for several reasons. First is that the largest energy difference between two quantum states in the QD that give rise to a true energy gap, and thus suppress phonon emission, are the lowest lying energy states of E_0 and E_1. This energy difference can be substantially larger than the optical phonon energy and is > 50 meV in many self-organized QDs. Therefore these lowest energy states will also exhibit the most efficient radiative emission. In addition, however, the states of E_0 and E_1 illustrated in Fig. 1 give rise to transverse electric field polarization, and surface emission. Therefore it is highly desirable to realize a QD unipolar heterostructure design that can effectively utilize these two lowest energy states in a QD and that have the height-to-base aspect ratio as shown in Fig. 1. Moreover, this aspect ratio is common to self-organized QDs in which the base is often a factor of two or greater than the height.

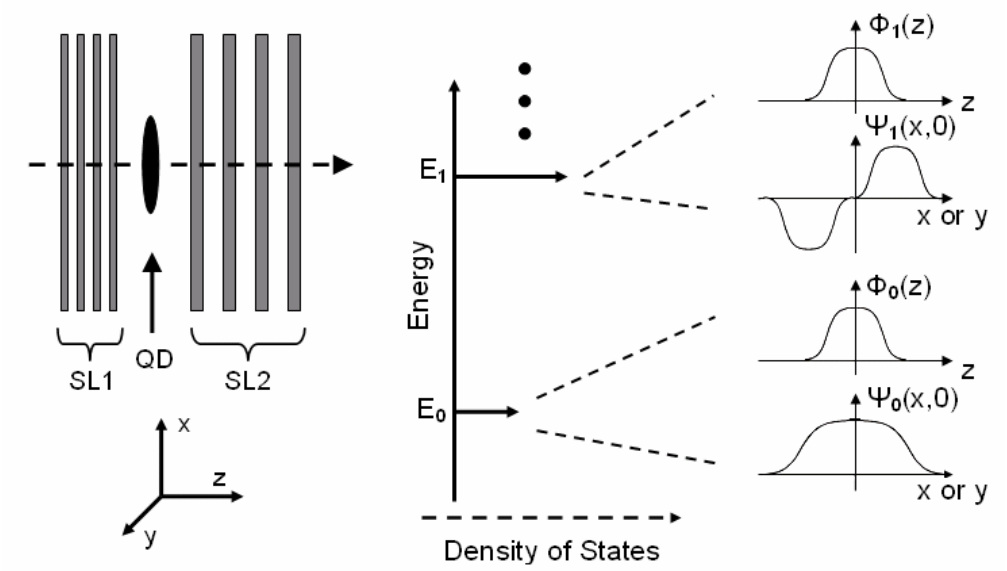

Figure 1: Schematic of a single QD between two superlattices (SL) and the illustration of its confined wavefunctions for the two lowest energy levels, E_0 and E_1. Because of the QD height-to-base aspect ratio, the two lowest energy levels exhibit the same z-dependence and are spatially orthogonal in the x-y plane. In this situation it is not possible to design SL1 and SL2 to achieve electronic confinement to the QD.

Figure 2 illustrates a new design that again uses a bulk barrier to inject and confine electrons on the injection side of the gain stage, and a tunnel barrier to deplete the lower gain level. This approach now also uses a second QD designed to solve the problem of the wavefunction symmetries discussed for Fig. 1 and achieve quasi-three-dimensional quantum confinement to the upper and lower energy levels of the gain stage. Instead of relying on a superlattice injector, the energy relaxation of electrons and capture into QD1 can occur over the bulk heterobarrier much as occurs for carrier capture in an electron hole laser. On the other hand, tunnelling is ultimately used for depletion of the lower electron level of the QD gain stage and apparently still required for the unipolar approach. The design uses two QDs with light emission obtained from QD1 while the quantum states of QD2 are engineered to provide the electronic confinement needed to efficiently excite the radiative transitions in QD1.

The quasi-three-dimensional quantum confinement is achieved by engineering both the composition and the aspect ratio of QD2 to create the energy level diagram illustrated on the right in Fig. 2. Achieving this aspect ratio in actual self-organized QDs is discussed in more detail below. The second dot, QD2, is engineered to have wider energy spacings than QD1

due to its smaller size, and a larger In composition is used to obtain a deeper confinement level. This double dot stacking permits electron confinement in QD1. The tunnel barrier of QD2 plays an interesting role, blocking electrons that exist in the higher energy two-dimensional space of QD1 or QD2. The same tunnel barrier, on the other hand, is less effective at blocking electron tunnelling out of a quasi-zero-dimensional state due to the diffraction effects discussed above. Therefore, even a thick tunnel barrier that effectively blocks the electron flow for higher energy states in the wetting layers and above for QD1 and QD2 can pass the electron from the confined quantum state in the QDs. A quantum well is then used to deplete the lower energy level of the QD2 through the tunnel barrier.

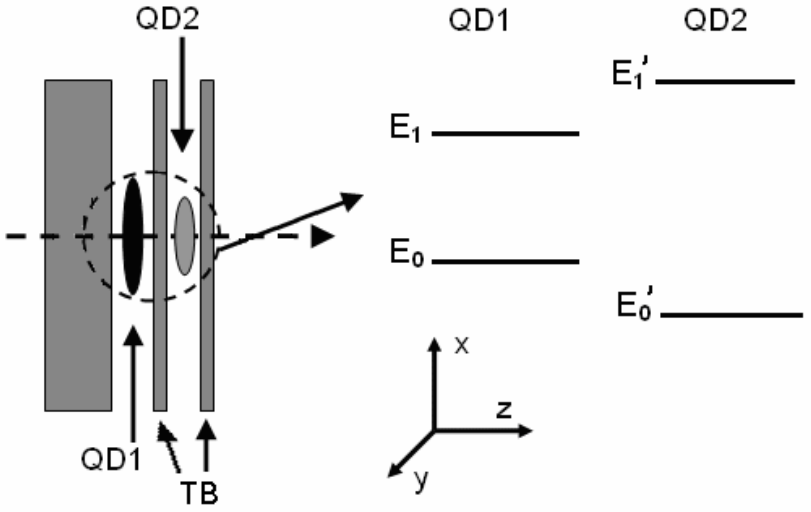

Figure 2: Schematic of a double quantum dot structure with their respective energy levels. The sizes and compositions of QD1 and QD2 are engineered to produce the energy structure shown on the right, with QD2 providing electronic confinement to QD1. The lower energy level E_0 of QD1 is depleted through relaxation into E_0' of QD2, and the electron escapes by tunnelling through the planar tunnel barrier (TB).

3. Actual QD Heterostructure Design and Growth

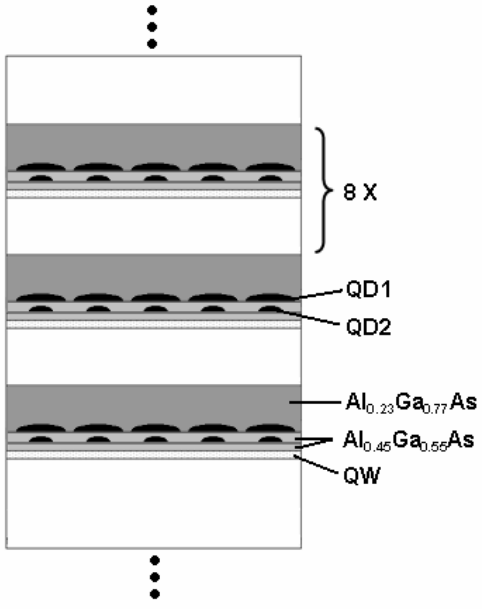

Figure 3: Schematic of the QD hetero-structure utilizing eight double QD gain

The structure proposed is composed of eight double QD gain stages and a GaAs waveguide. Each stage is undoped and is comprised of an injector region and an "active" QD, QD1, where the radiative transition occurs, and a second QD, QD2, that confines the electron to the radiative transition. The stage is formed by two QD layers, AlGaAs barriers, and a quantum well. An energy band schematic is depicted in figure 4: the electron is injected into the first excited state of QD1, and relaxes to the ground state via a photon emission. It then tunnels through the AlGaAs barrier into the ground state of QD2 via phonon scattering, and finally into the quantum well. It is accelerated in the injector region and the whole process starts over. In order for QD2 to have wider energy levels as well as a deeper confinement energy, both the lateral size and the In composition have been varied. A smaller diameter for QD2 is needed to

obtain wider energy spacing, while a higher In composition lowers QD2's ground state.

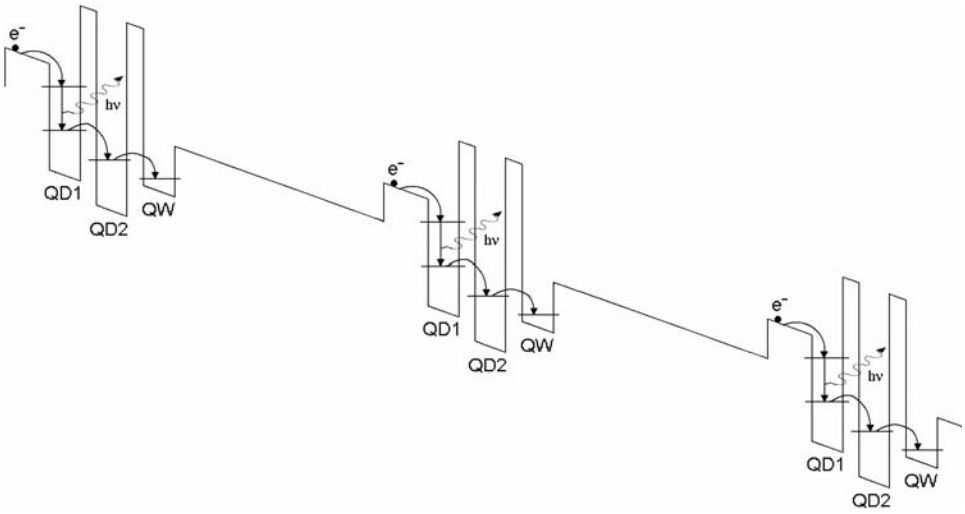

Figure 4: Energy band schematic showing the electron path in the active region of the 2 QD gain stages.

The structures are grown by molecular-beam epitaxy on n^+ GaAs substrates. The injector region is formed by a 200 nm GaAs and a 100 nm $Al_{0.23}Ga_{0.77}As$ layer. The two layers of dots are grown according to the Stranski-Krastanow growth mode by depositing 6 monolayers (MLs) of $In_{0.4}Ga_{0.6}As$ and 4.25 MLs of $In_{0.5}Ga_{0.5}As$ for QD1 and QD2 respectively. The dot layers are separated by a 7 nm $Al_{0.45}Ga_{0.55}As$ barrier. Due to the reduced size of this barrier and the fact that the first dot layer induces strain fields, a preferred direction for In migration occurs. This leads to vertically aligned dots with the larger diameter dots forming on the top of the smaller diameter dots. A 7 nm $Al_{0.45}Ga_{0.55}As$ barrier separates the second dot layer from the 9 nm $In_{0.2}Ga_{0.8}As$ quantum well. The GaAs waveguide is composed of two layers with different doping concentrations: a 3.5 µm GaAs layer ($n_{Si} = 4x10^{16}$ cm^{-3}) located above and below the 8 active region stages, and a 1 µm GaAs layer ($n_{Si} = 4x10^{18}$ cm^{-3}) to complete the waveguide cladding. Using Al-free waveguide avoids the instabilities on device thresholds and slope efficiencies produced by AlGaAs layers and yields a better thermal conductivity [6].

The first QD layer is grown using bulk deposition at 495°C, while sub-monolayer deposition at 515°C is used for the second layer. Those variations in growth techniques are needed to obtain the lateral size variation required. The growth was monitored by a Reflection High Energy Electron Diffraction (RHEED) system. The dot formation was signalled by an abrupt change in the RHEED pattern, which changes from streaky to spotty. Both dot layers have been found to form around 4 ML. Two uncapped samples containing the first dot layer and both layers are grown under the similar conditions for atomic force microscopy (AFM) measurements, with the AFM images shown in Figs. 5 and 6. The dot heights and spatial representations obtained from figure 5 are depicted in figure 6. The average diameters of the first and second dot layers are ~15 nm and ~30 nm respectively. Both layers exhibit an average height of ~7 nm and an average density of $2.5x10^{10}$ dots/cm^2.

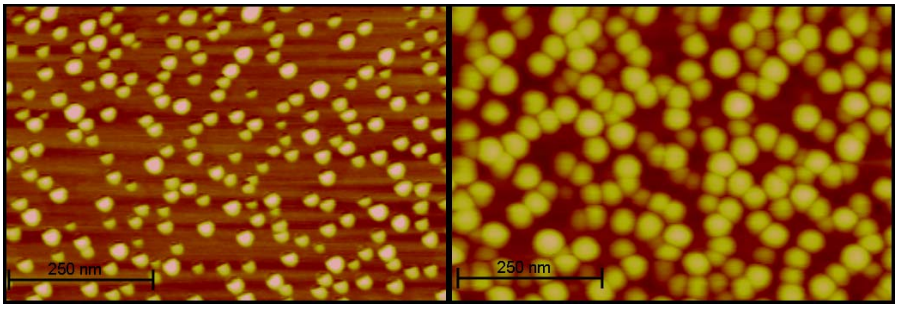

Figure 5: AFM picture of QD1 (left) and QD2 (right) layers

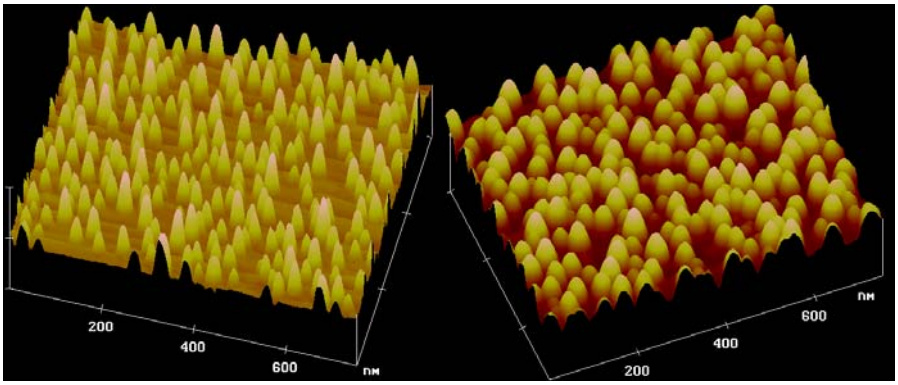

Figure 6: Spatial representation of QD1 (left) and QD2 (right) layers

4. Processing and First Measurements

Those QD cascade laser structures are processed as edge-emitting ridge waveguide devices. An n back contact consisting of a stack of Au-Ge/Ni/Au layers is first evaporated. Au-Ge forms alloy with GaAs while Ni acts as a diffusion barrier. Au is used as the upper contact layer due to its better electrical conductivity and stability. 100 µm wide windows are patterned using optical lithography and a second n contact similar to the back contact is evaporated in the openings. After lift-off, the metal stripes are protected by 400 µm wide photoresist stripes and the devices are etched down to the substrate using an isotropic aqueous solution of H_2SO_4:H_2O_2:H_2O (1:4:40). The etch rate is about 9 nm/s. This wet etching leads to very smooth and continuous sidewalls, marked by approximately 45° slopes. The last processing step is the thermal annealing of both n contacts at 420°C for 30 s. During this process, the Ge atoms of the Au-Ge alloy diffuse into the GaAs layer to form a low resistance ohmic contact. Once the samples have been processed, they are cleaved into waveguides of approximately 1 mm length.

The current-voltage characteristic of the devices (Fig. 7) exhibits a turn-on voltage of about 6 V, due to the large resistance resulting from the 2.5 µm undoped active region. Electroluminescence measurements are currently in progress with the samples being mounted for placement in a cryostat.

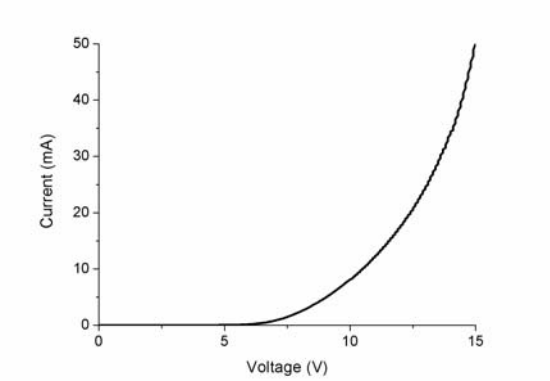

Figure 7: Current-voltage characteristics of the devices

5. Conclusions

In conclusion, we propose and demonstrate the epitaxial growth of a new heterostructure based on stacking two QDs of different lateral size for QDCLs. Compared to previously proposed structures, the new QD heterostructure is capable of confining electrons in quasi-zero-dimensional states to obtain intersubband transitions from the lower two energy levels with transverse electric polarization. This could lead to surface emission that would be very valuable in VCSELs and to the realization of the first quantum dot cascade laser

6. Conclusions

This research has been supported by the Army Research Office under grant number W911NF-04-1-0313.

7. References

[1] J. Faist, F. Capasso, D. Sivco, C. Sirtori, A. L. Hutchinson, and A. Y. Cho, Science **264**, 553 (1994)
[2] J. Faist, F. Capasso, C. Sirtori, D. Sivco, A. L. Hutchinson, S-N. G. Chu, and A. Y. Cho, Appl. Phys. Lett. **64**, 1144 (1994)
[3] S. Krishna, P. Bhattacharya, J. Singh, T. Norris, J. Urayama, P. J. McCann, and K. Namjou, IEEE J. Quantum Electron. **37**, 1066 (2001)
[4] N. Ulbrich, J. Bauer, G. Scarpa, R. Boy, D. Schuh, and G. Abstreiter, S. Schmult and W. Wegschneider, Appl. Phys. Lett. **83**, 1530 (2003)
[5] C-F. Hsu, J-S. O, P. Zory, and D. Botez, IEEE J. Select. Topics Quantum Electron. **6**, 491 (2000)
[6] C. Sirtori, P. Kruck, S. Barbieri, H. Page, J. Nagle, M. Beck, J. Faist, and U. Oesterle, Appl. Phys. Lett. **75**, 3911 (1999)